Contents lists available at GrowingScience

Engineering Solid Mechanics

homepage: www.GrowingScience.com/esm

Mechanical behavior evaluation and degradation mechanism for HMPE yarns under fatigue abrasion tests

Eduarda da Silva Belloni[a], Daniel Magalhães da Cruz[b*] and Carlos Eduardo Marcos Guilherme[c]

[a]*Federal Center for Technological Education Celso Suckow da Fonseca (CEFET-RJ), 23812-101, Itaguaí/RJ, Brazil*
[b]*Applied Mechanics Group (GMAp), Department of Mechanical Engineering (DEMEC), Federal University of Rio Grande do Sul (UFRGS), 90050-170, Porto Alegre/RS, Brazil*
[c]*Stress Analysis Laboratory Policab, Engineering School (EE), Federal University of Rio Grande (Furg), 96203-000, Rio Grande/RS, Brazil*

ARTICLE INFO

Article history:
Received 5 April 2024
Accepted 22 July 2024
Available online
22 July 2024

Keywords:
High Modulus Polyethylene Fibers
Offshore Mooring
Yarn-on-Yarn Abrasion
Mechanical Behavior
Environmental Degradation
Scanning Electron Microscopy (SEM) Analysis

ABSTRACT

Offshore oil exploration in deeper waters has necessitated the development of lighter mooring systems to replace traditional steel cable and chain platforms. This study focuses on evaluating the mechanical behavior and fatigue degradation mechanism of high modulus polyethylene (HMPE) fibers in yarn-on-yarn abrasion tests. Initial characterization tests, including linear density, rupture force, and thermal analysis, were conducted on HMPE yarns. Yarn-on-yarn abrasion tests were performed under dry, wet, and salty conditions, with varying loads, while statistical analysis examined the influence of environmental factors and load levels on yarn performance. Scanning electron microscopy (SEM) analysis provided insights into material degradation mechanisms. Results showed superior performance in freshwater-immersed yarns due to cooling and lubrication effects, while dry conditions led to material melting. SEM analysis revealed critical degradation zones, particularly in interwoven regions, where increased friction and heat concentration caused material fusion. Degradation evolution mechanisms highlighted fatigue-induced rupture of yarns, knot formation, and material melting near failure points. This comprehensive analysis enhances understanding of HMPE yarn performance and degradation in offshore mooring applications, laying the groundwork for developing advanced mooring systems capable of withstanding deep-sea environments.

1. Introduction

Over the past few decades, offshore oil fields have been increasingly explored in deeper waters, leading the oil and gas industry to replace traditional steel cable and chain platform anchor systems (Bastos *et al*., 2016). Oil reserves found in the pre-salt layer off the Brazilian coast, for example, have depths ranging from 1000 to 2000 meters (Beltrao *et al*., 2009; Costa Fraga *et al*., 2014; Wenyuan *et al*., 2023). At these depths, the weight of steel cables and chains would exceed the floating forces of the platform. To overcome this problem, the industry has developed lighter mooring systems based on polymeric materials (Del Vecchio, 1992; Weller *et al*., 2015; Arias *et al*., 2016). Thus, synthetic fiber ropes such as high modulus polyethylene (Marissen, 2011; Vlasblom *et al*., 2012; Han *et al*., 2016; Humeau *et al*., 2018; Lemstra, 2022), polyester (Huang *et al*., 2015; Xu *et al*., 2021; Nguyen & Thiagarajan, 2022; da Cruz *et al*., 2023a), liquid crystal polymer (Al Christopher *et al*., 2021; Galinski *et al*., 2022), polyamide (Chevillotte *et al*., 2020; Civier *et al*., 2022; Cruz *et al*., 2023), and aramid (Huang *et al*., 2015; Jassal *et al*., 2020) were introduced due to their smaller diameter for the same strength. These materials have excellent properties such as easy handling, storage, and transport, better resistance to fatigue and flexion, UV, and chemical resistance (Karayaka *et al*., 1999; Mckenna *et al*., 2004; Vannucchi de Camargo *et al*., 2016; Davies *et al*., 2011).

* Corresponding author.
E-mail addresses: daniel.cruz@ufrgs.br (D.M. da Cruz)

ISSN 2291-8752 (Online) - ISSN 2291-8744 (Print)

doi: 10.5267/j.esm.2024.7.002

Polyester ropes are widely used for deepwater mooring nowadays (Bastos *et al*., 2016; Umana *et al*., 2022). Among their main advantages are low production costs and hydrophobic properties. Conversely, the relatively low material stiffness becomes a problem in conventional anchoring systems (Kim *et al*., 2021; Xu *et al*., 2021; Huang *et al*., 2023). In comparative terms, polyester ropes have a break length of 10% - 11% (Weller *et al*., 2015; da Cruz *et al*., 2022; Melito *et al*., 2023), while high modulus polyethylene ropes typically have a break length of 2% - 3.5% for a worked rope (Weller *et al*., 2015; da Cruz *et al*., 2022). This outstanding high stiffness makes HMPE an excellent candidate for anchor system cables. In fact, the development of HMPE ropes is relatively recent, and the literature is somewhat scarce. Some recent studies have performed tensile fatigue tests on a series of fibers commonly used in offshore anchorages. The tests were conducted in dry conditions, and it was found that HMPE and aramid have higher tensile strength and fatigue resistance (Davies *et al*., 2011; Humeau *et al*., 2018). However, when fatigue tests were performed on wet materials, the HMPE presented higher fatigue strength than the others (Humeau *et al*., 2018). In another article, the fatigue strength study was conducted by varying temperatures (Lian *et al*., 2017), and it was concluded that as temperature increased, there was a loss of resistance to cyclic loading even in wet conditions, probably due to the near melting point of the material (150°C) because the toughness and fiber modulus decreased at high temperatures. Although the rope samples did not show excessive internal abrasion or debris from abrasion, fibrillation, and tapered filaments indicated a mechanism of plastic creep failure (Lian *et al*., 2018; da Cruz *et al*., 2023b). However, to understand the friction of polymer fibers, an abrasion test must be done (ASTM, 2016; Sheng *et al*., 2021).

There are three known types of failure under tension fatigue loading: failures caused by creep phenomena, external abrasion, or internal abrasion (Barrois, 1979; Vlasblom *et al*., 2017; Davies & Verbouwe, 2018; Davies & Arhant, 2019). Creep failures cause material plastic deformation to rupture, while abrasion failures are caused by friction of the yarns rope (internal abrasion) or by friction of the ropes with mooring materials (external abrasion) (Humeau *et al*., 2018). If the failure is governed by creep, the failure time will be independent of the testing frequency, depending only on the time spent under load. Thus, models for static creep strain prediction can be used, thereby replacing constant load with cyclic load (Vlasblom *et al*., 2017; Davies & Verbouwe, 2018).

However, during dynamic loading, all three phenomena can occur simultaneously. Under conditions of low amplitude and high cycle, yarn-yarn abrasion and hysteresis heating contribute significantly to damage accumulation (Zhao *et al*., 2019). Internal abrasion of fiber surfaces leads to fretting fatigue and increases the rope temperature. Creep deformation may be enhanced due to hysteresis heating of the ropes. Damage accumulation contributes to rope failure (Davies & Arhant, 2019), and this phenomenon can induce deviations from this type of prediction. In this case, the study of the type of failure and its location allows the type of friction involved to be identified.

Currently, the literature on studies of the behavior of polymeric fibers (and composites) in marine applications suggests the use of Scanning Electron Microscopy (SEM) (Jariwala & Jain, 2019; Jesthi & Nayak, 2019; Demircan *et al*., 2023) due to its peculiar advantages, such as a large depth of field and fine lateral resolution. This microscopy has the advantage of combining images obtained through the secondary electron signal (topography and morphology) with images obtained by backscattered electron signal (contrasts in compositions), which allows us to understand the evolution of degradation or wear mechanisms locally, according to the mechanical tests. The main objective of this study is to evaluate the mechanical behavior and fatigue degradation mechanism of high modulus polyethylene fibers in abrasion tests (Yarn-on-Yarn). Mechanical tests were performed on the materials in three different atmospheres: dry, wet, and salty. Abrasion tests were performed following the ASTM D6611 standard (ASTM, 2016). In addition, an analysis of the degradation evolution was performed by scanning electron microscopy (SEM).

2. Materials and Methods

2.1 Material and Initial Characterization Tests

High modulus polyethylene yarns supplied by company Petrobras was used, they are utilized for ropes manufacturing (**Fig.** 1). An initial mechanical characterization is made in terms of linear density, rupture (Yarn Break Load) and linear tenacity. The linear density follows the ASTM D1577 standard (ASTM, 2018), using a series of measurements on a precision scale with a stabilization time of 9 minutes per sample, obtaining the linear density of the material in units [tex] which is the same as [g/km] for 30 samples. For the Yarn Break Load (YBL) test, the ISO 2062 standard is followed (ISO, 2009), with a useful length (between clamping claws) of 500 mm and speed of 250 mm/min for breaking, obtaining breaking force values in [N] and rupture length in [mm] for 30 samples. Linear tenacity is obtained mathematically by dividing the rupture value by the linear density value, resulting in the unit [N/tex].

All mechanical initial characterization tests meet the standard atmosphere norm for fiber testing (ISO, 2005), with a temperature of 20 ± 2°C and relative humidity of 65 ± 4%. Finally, still for material characterization, but for a thermal-chemical approach, Differential Scanning Calorimetry (DSC) and ThermoGravimetric Analysis (TGA) were carried out, where the objective is to obtain information through monitoring heat flow as a function of temperature, regardless of the occurrence or not of mass variation. DSC analysis was performed using a Shimadzu DSC – 60 calorimeters, with a temperature

range of 25 °C to 300 °C, heating rate of 10°C/min (ASTM, 2020). The sample's thermogravimetric (TG) curves were obtained on a Shimadzu TGA-60 thermobalance model with a heating rate of 10°C/min, where the samples were placed in aluminum pans and heated from 35°C to 550°C (ASTM, 2016).

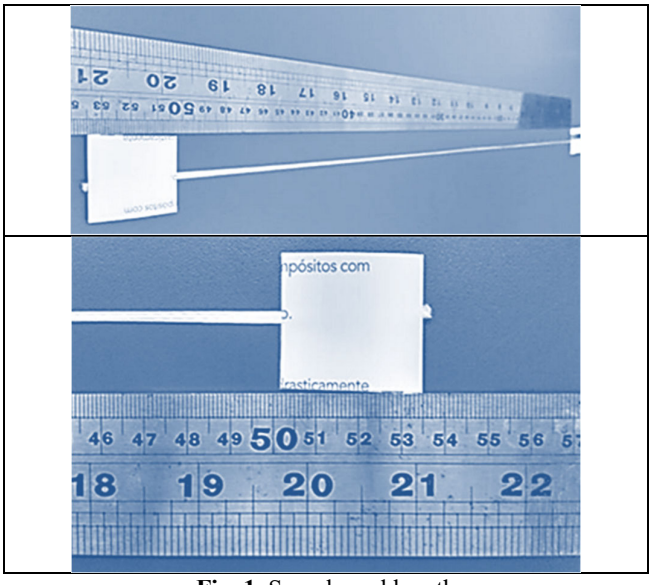

Fig. 1. Sample and length

2.2 Yarn-on-Yarn Abrasion

2.2.1 Test Conditions and Sample Preparation

The samples are tested in three different atmospheres: Dry, wet and salty. Considering the following the conditions (CI, 2009):

- Dry Testing: The tests were performed in an atmosphere with a relative humidity of 65 ± 4 % and 20 ± 2°C temperature.
- Wet Testing: In preparation for wet testing, each sample were preconditioned to a fresh tap water bath at 20 ± 2°C temperature for 60 ± 5 min. Besides, during the test, the interwrapped region of the yarn was completely immersed.
- Salty Testing: In preparation for salty testing, each sample were preconditioned to a seawater bath at 20 ± 2°C temperature for 60 ± 5 min. Besides, during the test, the interwrapped region of the yarn was completely immersed.

Sample preparation is carried out on a bench, with specimens approximately 800 mm long, and which have nodes at their ends for positioning in a crank and tension weight.

2.2.2 Mechanical Test and Load Conditions

The yarn-on-yarn abrasion test was performed as described in norm by Cordage Institute: “Method for Yarn-on-Yarn Abrasion” and in norm by American Society for Testing and Materials: “Standard Test Method for Wet and Dry Yarn-on-Yarn Abrasion Resistance”. This method consists of twisting the filaments around themselves and stretching with a pre-established load. This load forces cause friction between the filaments during the machine cycles.

For this type of method, the equipment used was developed by the Stress Analysis Laboratory Policab according to established standards (CI, 2009; ASTM, 2016). The superior pulleys are 140 mm distant, and the lower pulley is 254 ± 2 mm distant from the others, producing a 34° angle for the arrangement. The engine thrust rotate at 60 rpm and the yarn should have three full turns, producing an interwrapped region of 1080° (**Fig. 2**). Besides, the machine was programmed to record the number of cycles to failure.

Fig. 2 shows de mechanism for a dry test material. For the wet and salty test, the interwrapped yarn region is completely immersed in a beaker of freshwater and seawater, respectively. Considering the standard recommendation selected loads were applied. For each condition (dry, wet and salty), abrasion tests were carried out for 3 different loads: 2%, 4% and 6% of the

Yarn Break Load (YBL). About quantities, there are 10 samples per "condition-load" group, totaling 90 samples for Yarn-on-Yarn test.

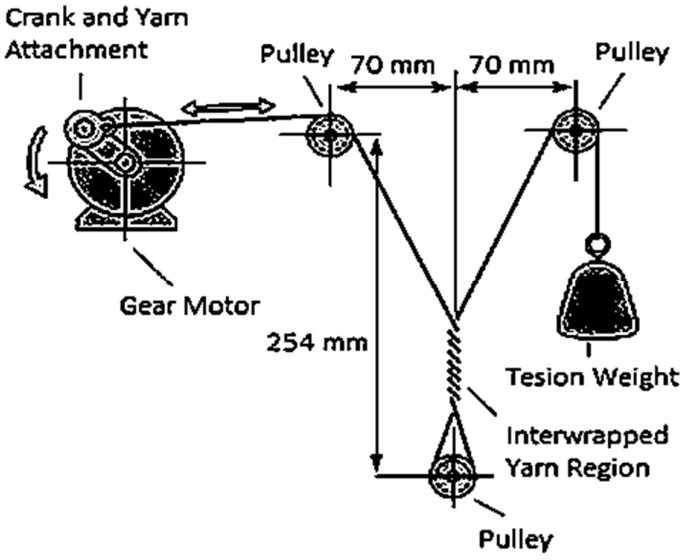

Fig. 2. General Arrangement of the Yarn-on-Yarn Abrasion Test

2.2.3 Statistic Analysis

The method used to calculate the geometric mean cycles to failure and number of cycles standard deviation to failure was followed by ASTM D6611 recommendation.

To analyze the influence of the factors effect on the number of cycles to failure, was used the analysis of variance (ANOVA). In the analysis three null hypotheses were verified:

- $H_0(A)$: $\tau_1 = \tau_2 = \tau_3 = 0$, (there is no difference in the number of cycles until the rupture for the different atmospheres);
- $H_0(B)$: $\beta_1 = \beta_2 = \beta_3 = 0$, (there is no reduction in the number of cycles until rupture when increasing load); and
- $H_0(AB)$: $(\tau\beta)_{ij} = 0$ (there is no interaction between the atmosphere and load).

Using 95% confidence interval, p-value is calculated for each of the three statistical tests. If p-value ≤ 1%, the null hypothesis is rejected, and if p-value ≥ 1% the null hypothesis is accepted (Marôco, 2012; Montgomery, 2017).

2.2.4 Scanning Electron Microscope Analysis

For Yarn-on-Yarn tests, the surface of high modulus polyethylene is investigated in the abrasion region using a Scanning Electron Microscope (SEM) TM 400 – Hitachi model. To analyze the degradation of the material along the interlaced yarns region, a qualitative analysis was carried out. The interlaced region varied from 60 mm to 70 mm depending on loading conditions and atmosphere.

This region was sectioned into 4 parts and analyzed as shown in **Fig. 3**. Amplifications of 100x and 200x were used for the analysis, considering the atmospheres mentioned (dry, wet and salty), and for cycling conditions: 1/3 cycle to failure, 2/3 cycle to failure, and sample after abrasion failure.

3. Results and Discussions

3.1 Mechanical Characterization

The mean results for the initial mechanical characterization in terms of linear density, rupture force, rupture strain and linear tenacity are shown in Table 1. Among the values shown, it is worth highlighting the linear tenacity value being greater than 2.5 N/tex, meeting the requirement of ISO 18692-3 for high performance HMPE fiber (ISO, 2019).

Table 1. Mechanical characterization results

Linear Density [tex]	Yarn Break Load [N]	Extension at Break [mm]	Strain at Break [%]	Linear Tenacity [N/tex]
176.4 ± 8.3	502.11 ± 7.42	15.70 ± 2.85	3.14 ± 0.57	2.846 ± 0.185

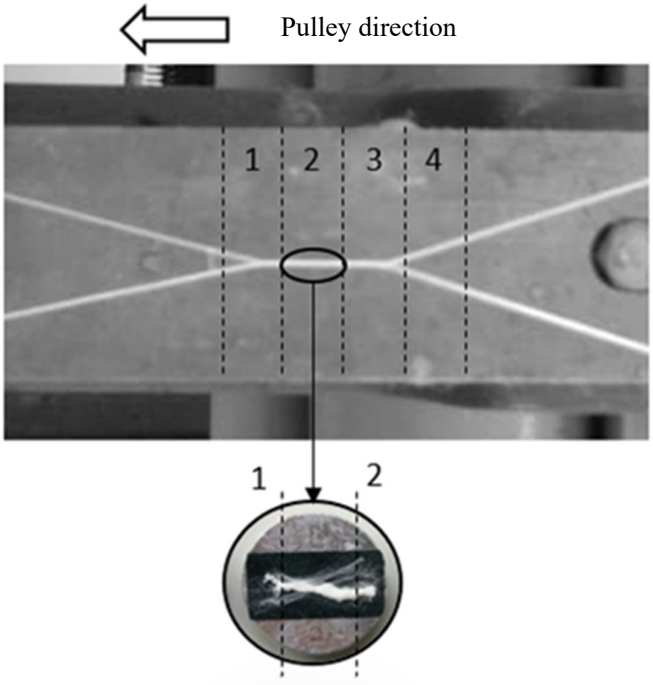

Fig. 3. SEM analysis methodology

Fig. 4 presents the discrete rupture data for the 30 tested samples, in terms of rupture force [N] and strain [mm/mm]. Furthermore, **Fig. 5** presents the average stress-strain curve for the data set.

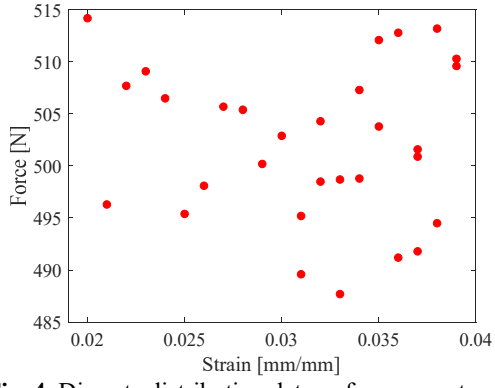

Fig. 4. Discrete distribution data, reference rupture test

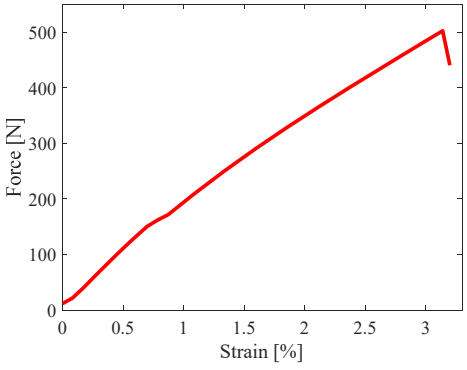

Fig. 5. Constitutive curve, force *versus* strain.

The tests indicated in section 2.2 for yarn-on-yarn abrasion fatigue use this rupture result as a reference. As previously stated, 3 load conditions are explored, 2%, 4% and 6% of the breaking load. This percentage can be expressed in force [N], and also in masses [kg] (weights that will be used in the abrasion equipment). **Table 2** presents the reference values (100% of YBL) and for 2%, 4% and 6% in relation to force and mass.

Table 2. Loads for yarn-on-yarn tests

[%YBL]	Force [N]	Mass [kg]
100%	502.11	51.20
2%	10.042	1.024
4%	20.084	2.048
6%	30.127	3.072

3.2 Thermal Characterization

Fig. 6 shows the thermogravimetric (TGA) and differential scanning calorimetry (DSC) curves in inert atmosphere. For TGA, the indication is represented in blue and dashed line with percentage of mass loss unit. Whereas for DSC, the indication is shown in red and continuous line with power unit (energy or heat per time).

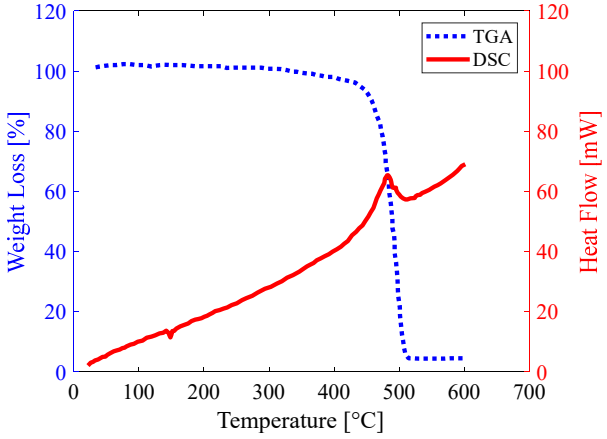

Fig. 6. Thermogravimetric (TGA) and differential scanning calorimetry (DSC) curves.

Differential scanning calorimetry (DSC) curve showed an endothermic peak in 147.18°C (420.33 K). At this point, the system energy provides the reduction of secondary intermolecular forces between the crystalline phase chains, changing from plastic state to viscous (fluid) state. In addition, an exothermic peak was observed at 481.67°C (754.82 K), leading to a polymeric chain degradation. This thermal behavior can also be observed in the mass loss, as demonstrated in the thermogravimetric curve.

3.3 Yarn-on-Yarn Test Results

Yarn-on-yarn testing was performed until failure, which occurred in the interwoven section of the multifilament in all reported cases, with results shown in Table 3 for mean and standard deviation (SD), for all atmosphere and load conditions.

Table 3. Number of cycles results for abrasion failure in the yarn-on-yarn test

Load [N]	Dry		Wet		Salty	
	Mean	SD	Mean	SD	Mean	SD
10.042	1602.50	2.46	2263.60	2.22	3842.20	2.49
20.084	132.80	3.52	325.50	3.03	974.10	3.67
30.127	6.80	1.32	83.50	2.27	441.50	3.03

Each result is the mean of 10 samples, something that stands out in the results are the low standard deviations. Other works that address abrasion tests present considerable deviations (Bain *et al*., 2023; Cruz *et al*., 2024). It is possible to observe superior results obtained with immersed yarn in freshwater compared to the others; this occurs due to cooling and lubrication caused by water. Although seawater is highly corrosive, the material has better characteristics after its immersion, an effect also caused by cooling and lubrication of the yarns, but worse than freshwater, probably seawater, as it contains salts and small particles in suspension, intensifies the abrasion process in the intertwining region, reducing the number of resistant cycles in the abrasion test.

Fig. 7 graphically presents the discrete data from Table 3, in terms of number of cycles for rupture *versus* load. Furthermore, the same figure plots approximations for each of the data using the power models. The power model was chosen because it presents the best coefficient of determination (R^2), in all cases the R^2 was greater than 0.99.

The model equations presented in **Fig. 7** are shown for the wet condition YoY_w in Eq. (1), for the salty condition YoY_s in Eq. (2), and for the dry condition YoY_d in Eq. (3). Where YoY is the number of cycles for failure in the Yarn-on-Yarn test, and F is the force used respectively in the abrasion test.

$$YoY_w = 361317.484 \cdot F^{-1.970} \quad (1)$$

$$YoY_s = 2272754.791 \cdot F^{-2.981} \quad (2)$$

$$YoY_d = 137060490.016 \cdot F^{-4.823} \quad (3)$$

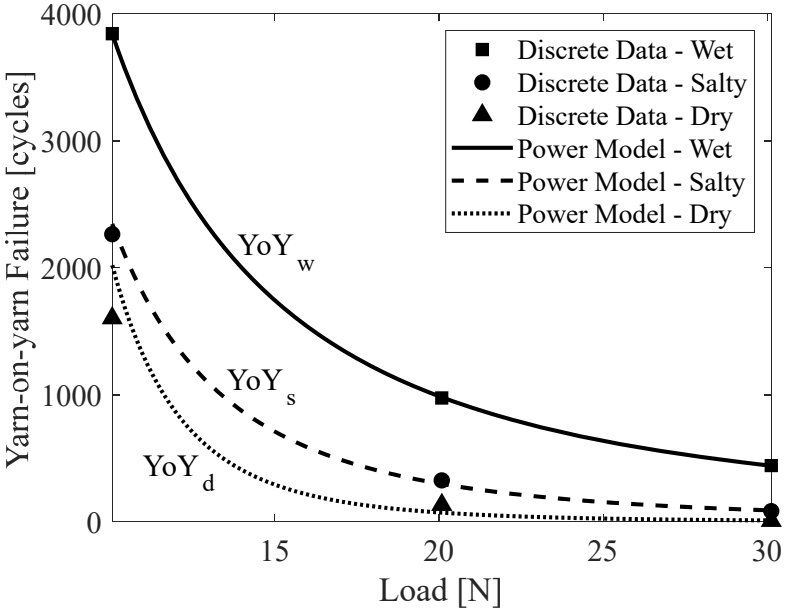

Fig. 7. Cycles to failure *versus* load.

The adopted mathematical criterion was the coefficient of determination, as mentioned earlier, in all cases it was greater than 0.99. However, it is important to highlight the exact value for each of the approximations: for the wet condition, $R_w^2 = 0.999996$; for the salty condition, $R_s^2 = 0.999683$, and for the dry condition, $R_d^2 = 0.998041$.

3.4 Degradation – SEM Analysis

3.4.1 Critical Zone

In this section, the critical zone with the highest degradation is presented and discussed. Only dry and wet conditions were compared, as salty did not show a significant difference from wet. It was observed that in Part 2, the highest degradation (**Fig. 8**) was obtained for both environments, likely due to the interwrapped region of the yarns, resulting in increased friction and heat concentration. In the dry environment, friction leads to material melting, causing several filaments to merge into a single thread. Meanwhile, in the wet environment, the fibers also melting, but to a lesser extent, due to the cooling effect and potential lubrication provided by the wet environment.

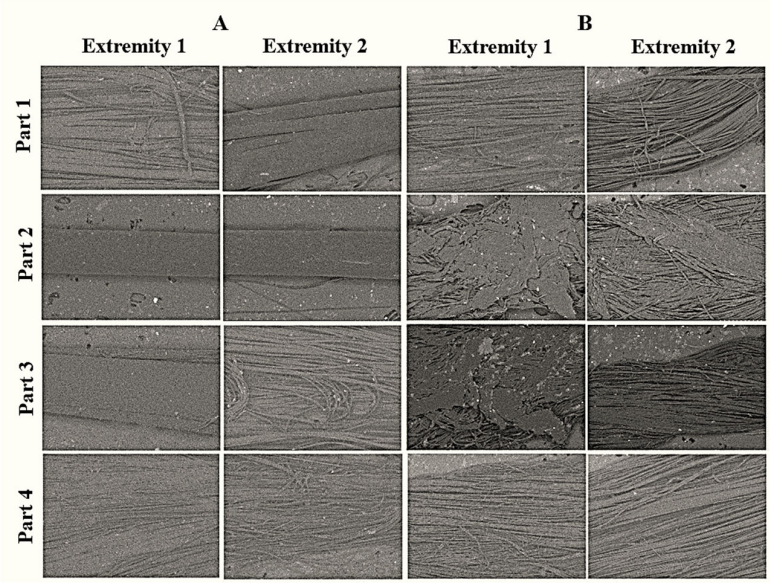

Fig. 8. Sample with 2% YBL and 1/3 cycles to failure: (A) Dry test; (B) Wet test.

Furthermore, the dry test material presented smaller diameter in part 2, while the wet test presented specific point knots degradation (**Fig. 8**), due to the peeling and material interlacing. The interwrapped region is the most affected, all samples ruptured in this region. However, a chemical analysis should also be conducted to observe whether heating the fibers results in the loss of any molecular components.

3.4.2 Degradation Evolution

In this section, the evolution of the degradation mechanism is discussed, considering 1/3 of the cycles until failure, 2/3 of the cycles until failure, and the fractured material. **Fig. 9** presents the critical zone (**Fig. 8**, Part 2) of the wet test, considering 4% YBL. Only the intermediate load of the tests was analyzed due to time of the research. It can be observed that the degradation mechanism due to fatigue primarily occurs through the rupture of some yarns, which interwoven with others, creating points of tension due to geometric differences.

Subsequently, this concentration of yarns ends up creating knots, causing the region to become abrasive, leading to the rupture of other yarns and increasing the region. Near the point of failure, the region where the concentration of broken yarns occurs begins to heat up, causing the melting of the material and consequently resulting in a loss of mechanical resistance and even failure.

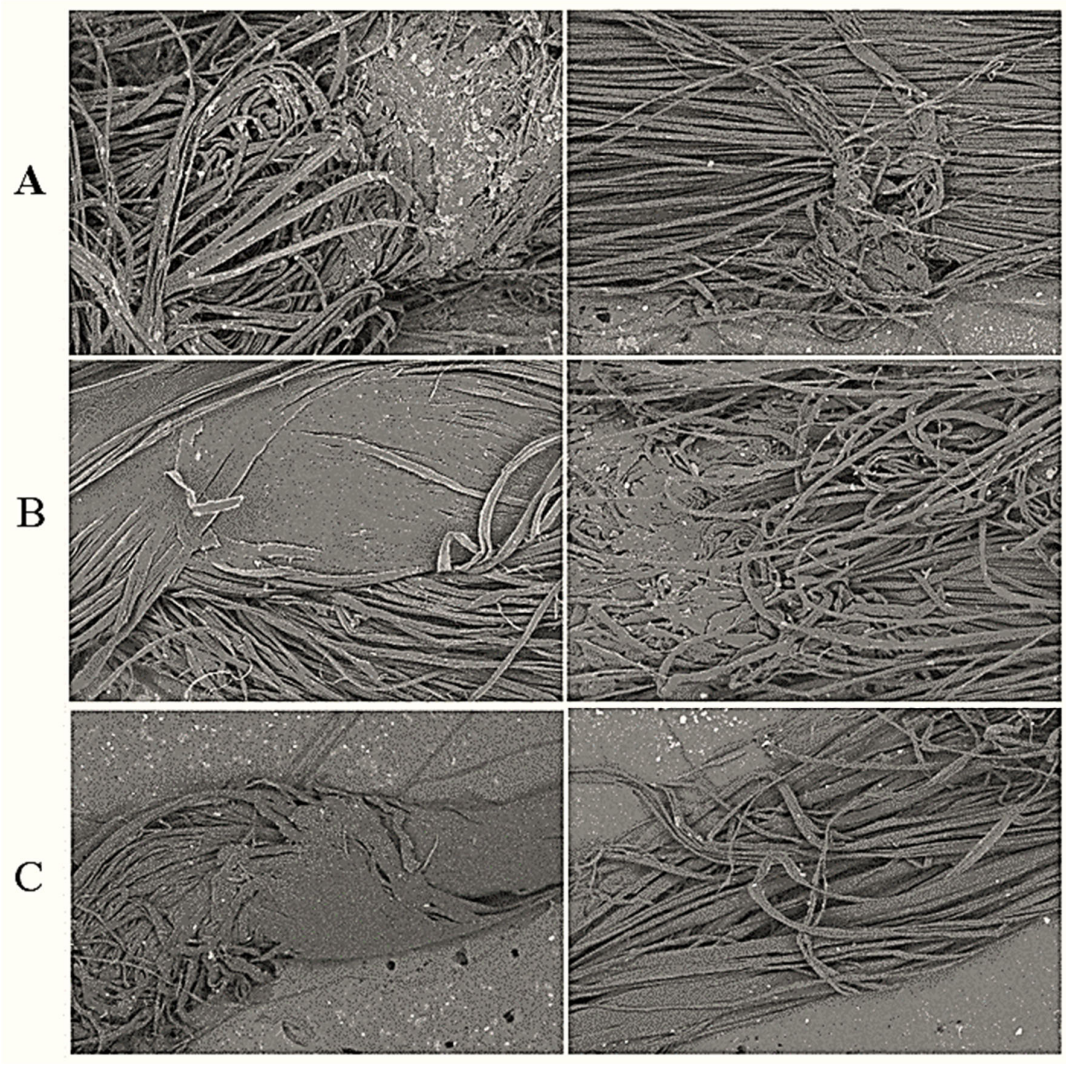

Fig. 9. Degradation evolution for 4% YBL: (A) 1/3 cycles to failure; (B) 2/3 cycles to failure and (C) Failure sample.

4. Conclusions

This analysis enhances our understanding of the performance and degradation of high modulus polyethylene (HMPE) yarns in offshore mooring applications. By pinpointing influential factors affecting material degradation, such as environmental conditions and load levels, it lays the foundation for developing advanced mooring systems capable of withstanding the rigors of deep-sea environments.

The study extensively investigated the properties of HMPE yarns, essential for rope manufacturing, through a comprehensive series of tests. Material characterization encompassed determining linear density, conducting tensile tests, and thermal analysis. Yarn-to-yarn abrasion tests were performed in dry, wet, and salty environments, each with specific loads and controlled temperature and humidity conditions. Statistical analysis meticulously evaluated the impact of these factors on yarn performance. Furthermore, scanning electron microscopy analysis provided valuable insights into material degradation in specific regions.

Yarn breaking load (YBL) tests, carried out via tensile tests on 30 virgin samples, established a baseline for subsequent assessments, as depicted in Table 1 and Fig. 4. Thermal characterization, illustrated in Fig. 6 through thermogravimetric (TGA) and differential scanning calorimetry (DSC) curves, unveiled significant thermal transitions, including an endothermic peak at 147.18°C and an exothermic peak at 481.67°C, indicating polymer chain degradation.

Yarn-on-yarn tests, detailed in Fig. 7, demonstrated superior performance in freshwater-immersed yarns, attributed to cooling and lubrication effects, while dry conditions yielded the poorest results, possibly due to material melting. Subsequent scanning electron microscope (SEM) analysis in section 3.4 revealed critical degradation zones, notably in Part 2, where increased friction and heat concentration in the interwrapped yarn region led to material fusion and filament merging.

Degradation evolution mechanisms, as discussed in section 3.4.2, elucidated fatigue-induced rupture of yarns, subsequent knot formation, and eventual material melting near failure points, emphasizing the intricate interplay between mechanical and environmental factors in yarn degradation.

Acknowledgments

This study was financed in part by the Coordenação de Aperfeiçoamento de Pessoal de Nível Superior - Brasil (CAPES) - Finance Code 001.

References

Al Christopher, C., da Silva, Í. G., Pangilinan, K. D., Chen, Q., Caldona, E. B., & Advincula, R. C. (2021). High performance polymers for oil and gas applications. *Reactive and Functional Polymers*, *162*, 104878. https://doi.org/10.1016/j.reactfunctpolym.2021.104878

American Society for Testing and Materials. (2016). D6611 *Standard Test Method for Wet and Dry Yarn-Yarn Abrasion Resistance*. ASTM: West Conshohocken. https://doi.org/10.1520/D6611-16

American Society for Testing and Materials. (2018). D1577 *Standard Test Methods for Linear Density of Textile Fibers*. ASTM: West Conshohocken. https://doi.org/10.1520/D1577-07R18

American Society for Testing and Materials. (2020). E1131 *Standard Test Method for Compositional Analysis by Thermogravimetry*. ASTM: West Conshohocken. https://doi.org/10.1520/E1131-20

Arias, R. R., Ruiz, Á. R., & de Lena Alonso, V. G. (2016). Mooring and anchoring. *Floating Offshore Wind Farms*, 89-119. https://doi.org/10.1007/978-3-319-27972-5_6

Bain, C., Davies, P., Riou, L., Marco, Y., Bles, G., & Damblans, G. (2023). Experimental evaluation of the main parameters influencing friction between polyamide fibers and influence of friction on the abrasion resistance. *The Journal of The Textile Institute*, *114*(7), 998-1006. https://doi.org/10.1080/00405000.2022.2105075

Barrois, W. (1979). Repeated plastic deformation as a cause of mechanical surface damage in fatigue, wear, fretting-fatigue, and rolling fatigue: a review. *International Journal of Fatigue*, *1*(4), 167-189. https://doi.org/10.1016/0142-1123(79)90022-7

Bastos, M. B., Fernandes, E. B., & da Silva, A. L. N. (2016). Performance fibers for deep water offshore mooring ropes: Evaluation and analysis. In *OCEANS 2016-Shanghai* (pp. 1-7). IEEE. https://doi.org/10.1109/OCEANSAP.2016.7485612

Beltrao, R. L. C., Sombra, C. L., Lage, A. C. V., Netto, J. R. F., & Henriques, C. C. D. (2009). SS: pre-salt Santos basin-challenges and new technologies for the development of the pre-salt cluster, Santos basin, Brazil. In *Offshore Technology Conference* (pp. OTC-19880). OTC. https://doi.org/10.4043/19880-MS

Chevillotte, Y., Marco, Y., Bles, G., Devos, K., Keryer, M., Arhant, M., & Davies, P. (2020). Fatigue of improved polyamide mooring ropes for floating wind turbines. *Ocean Engineering*, *199*, 107011. https://doi.org/10.1016/j.oceaneng.2020.107011

Civier, L., Chevillotte, Y., Bles, G., Montel, F., Davies, P., & Marco, Y. (2022). Short and long term creep behaviour of polyamide ropes for mooring applications. *Ocean Engineering*, *259*, 111800. https://doi.org/10.1016/j.oceaneng.2022.111800

Cordage Institute. (2009). 1503 *Test Method for Yarn-on-Yarn Abrasion*. CI: Wayne.

Costa Fraga, C. T., Lara, A. Q., Capeleiro Pinto, A. C., & Moreira Branco, C. C. (2014, June). Challenges and solutions to develop Brazilian pre-salt deepwater fields. In *World Petroleum Congress* (p. D033S003R004). WPC.

Cruz, D. M., Barreto, M. A., Zangalli, L. B., Cruz Júnior, A. J., Melito, I., Clain, F. M., & Guilherme, C. E. M. (2024). Mechanical characterization procedure of HMPE fiber for offshore mooring in deep waters. *Engineering Solid Mechanics*, *12*(3), 311-322. https://doi.org/10.5267/j.esm.2024.1.003

Cruz, D. M., Silva, A. H. M. F. T., Clain, F. M., & Guilherme, C. E. M. (2023). Experimental study on the behavior of polyamide multifilament subject to impact loads under different soaking conditions. *Engineering Solid Mechanics*, *11*(1), 23-34. https://doi.org/10.5267/j.esm.2022.11.001

da Cruz, D. M., Barreto, M. A., Zangalli, L. B., Popiolek Júnior, T. L., & Guilherme, C. E. M. (2023b). Experimental Study of Creep Behavior at High Temperature in Different HMPE Fibers Used for Offshore Mooring. In *Offshore Technology Conference Brasil* (p. D021S026R002). OTC. https://doi.org/10.4043/32760-MS

da Cruz, D. M., Clain, F. M., & Guilherme, C. E. M. (2022). Experimental study of the torsional effect for yarn break load test of polymeric multifilaments. *Acta Polytechnica*, *62*(5), 538–548. https://doi.org/10.14311/AP.2022.62.0538

da Cruz, D. M., Penaquioni, A., Zangalli, L. B., Bastos, M. B., Bastos, I. N., & da Silva, A. L. N. (2023a). Non-destructive testing of high-tenacity polyester sub-ropes for mooring systems. *Applied Ocean Research*, *134*, 103513. https://doi.org/10.1016/j.apor.2023.103513

Davies, P., & Arhant, M. (2019). Fatigue behaviour of acrylic matrix composites: influence of seawater. *Applied Composite Materials*, *26*(2), 507-518. https://doi.org/10.1007/s10443-018-9713-1

Davies, P., & Verbouwe, W. (2018). Evaluation of basalt fibre composites for marine applications. *Applied Composite Materials*, *25*(2), 299-308. https://doi.org/10.1007/s10443-017-9619-3

Davies, P., Reaud, Y., Dussud, L., & Woerther, P. (2011). Mechanical behaviour of HMPE and aramid fibre ropes for deep sea handling operations. *Ocean Engineering*, *38*(17-18), 2208-2214. https://doi.org/10.1016/j.oceaneng.2011.10.010

Del Vecchio, C. J. M. (1992). *Light weight materials for deep water moorings* (Doctoral dissertation, University of Reading).

Demircan, G., Ozen, M., Kisa, M., Acikgoz, A., & Işıker, Y. (2023). The effect of nano-gelcoat on freeze-thaw resistance of glass fiber-reinforced polymer composite for marine applications. *Ocean Engineering*, *269*, 113589. https://doi.org/10.1016/j.oceaneng.2022.113589

Galinski, H., Leutenegger, D., Amberg, M., Krogh, F., Schnabel, V., Heuberger, M., ... & Hegemann, D. (2020). Functional coatings on high-performance polymer fibers for smart sensing. *Advanced Functional Materials*, *30*(14), 1910555. https://doi.org/10.1002/adfm.201910555

Han, G., Tao, X., Li, X., Jiang, W., & Zuo, W. (2016). Study of the mechanical properties of ultra-high molecular weight polyethylene fiber rope. *Journal of Engineered Fibers and Fabrics*, *11*(1), 155892501601100103. https://doi.org/10.1177/155892501601100103

He, W., Shi, B., Fan, G., Wang, W., Wang, H., Wang., J., Zuo, G., Wang, C., & Yang, L. (2023). Theoretical and technical progress in exploration practice of the deep-water large oil fields, Santos Basin, Brazil. *Petroleum Exploration and Development*, *50*(2), 255-267. https://doi.org/10.1016/S1876-3804(22)60385-9

Huang, W., Li, B., & Kim, D. K. (2023). An investigation on material diversity of synthetic fiber ropes in the course stability of towing under wind. *Ocean Engineering*, *279*, 114410. https://doi.org/10.1016/j.oceaneng.2023.114410

Huang, W., Liu, H., Lian, Y., & Li, L. (2015). Modeling nonlinear time-dependent behaviors of synthetic fiber ropes under cyclic loading. *Ocean Engineering*, *109*, 207-216. https://doi.org/10.1016/j.oceaneng.2015.09.009

Humeau, C., Davies, P., Smeets, P., Engels, T. A. P., Govaert, L. E., Vlasblom, M., & Jacquemin, F. (2018). Tension fatigue failure prediction for HMPE fibre ropes. *Polymer Testing*, *65*, 497-504. https://doi.org/10.1016/j.polymertesting.2017.12.014

International Organization for Standardization. (2005). 139 *Textiles — Standard atmospheres for conditioning and testing*. ISO: Geneva.

International Organization for Standardization. (2009). 2062 *Textiles — Yarns from packages — Determination of singleend breaking force and elongation at break using constant rate of extension (CRE) tester*. ISO: Geneva.

International Organization for Standardization. (2020). 18692-3 *Fibre ropes for offshore stationkeeping — Part 3: High modulus polyethylene (HMPE)*. ISO: Geneva.

Jariwala, H., & Jain, P. (2019). A review on mechanical behavior of natural fiber reinforced polymer composites and its applications. *Journal of Reinforced Plastics and Composites*, *38*(10), 441-453. https://doi.org/10.1177/0731684419828524

Jassal, M., Agrawal, A. K., Gupta, D., & Panwar, K. (2020). Aramid fibers. *Handbook of fibrous materials*, 207-231. https://doi.org/10.1002/9783527342587.ch8

Jesthi, D. K., & Nayak, R. K. (2019). Evaluation of mechanical properties and morphology of seawater aged carbon and glass fiber reinforced polymer hybrid composites. *Composites Part B: Engineering*, *174*, 106980. https://doi.org/10.1016/j.compositesb.2019.106980

Karayaka, M., Srinivasan, S., & Wang, S. S. (1999). Advanced design methodology for synthetic moorings. In *Offshore Technology Conference* (pp. OTC-10912). OTC. https://doi.org/10.4043/10912-MS

Kim, K., Kim, T., Kim, N., Kim, D., Kang, Y., & Kim, S. (2021). Evaluating the mechanical properties of fiber yarns for developing synthetic fiber chains. *Journal of Ocean Engineering and Technology*, *35*(6), 426-433. https://doi.org/10.26748/KSOE.2021.072

Lemstra, P. J. (2022). High-performance polyethylene fibers. *Advanced Industrial and Engineering Polymer Research*, *5*(2), 49-59. https://doi.org/10.1016/j.aiepr.2022.03.001

Lian, Y., Liu, H., Zhang, Y., & Li, L. (2017). An experimental investigation on fatigue behaviors of HMPE ropes. *Ocean Engineering*, *139*, 237-249. https://doi.org/10.1016/j.oceaneng.2017.05.007

Lian, Y., Zheng, J., Liu, H., Xu, P., & Gan, L. (2018). A study of the creep-rupture behavior of HMPE ropes using viscoelastic-viscoplastic-viscodamage modeling. *Ocean Engineering*, *162*, 43-54. https://doi.org/10.1016/j.oceaneng.2018.05.003

Marissen, R. (2011). Design with ultra strong polyethylene fibers. *Materials Sciences and Applications*, *2*(05), 319. https://doi.org/10.4236/msa.2011.25042

Marôco, J. (2018). *Análise Estatística com o SPSS Statistics.: 7ª edição*. ReportNumber, Lda.

McKenna, H. A., Hearle, J. W. S., & O'Hear, N. (2004). *Handbook of fibre rope technology* (Vol. 34). Woodhead publishing.

Melito, I., Cruz, D. M., Belloni, E. S., Clain, F. M., & Guilherme, C. E. M. (2023). The effects of mechanical degradation on the quasi static and dynamic stiffness of polyester yarns. *Engineering Solid Mechanics*, *11*(3), 243-252. https://doi.org/10.5267/j.esm.2023.4.001

Montgomery, D. C. (2017). *Design and analysis of experiments*. John wiley & sons.

Nguyen, N., & Thiagarajan, K. (2022). Nonlinear viscoelastic modeling of synthetic mooring lines. *Marine Structures*, *85*, 103257. https://doi.org/10.1016/j.marstruc.2022.103257

Sheng, C., He, G., Hu, Z., Chou, C., Shi, J., Li, J., Meng, Q., Ning, X., Wang, L. & Ning, F. (2021). Yarn on yarn abrasion failure mechanism of ultrahigh molecular weight polyethylene fiber. *Journal of engineered fibers and fabrics*, *16*, 15589250211052766. https://doi.org/10.1177/15589250211052766

Umana, E. C., Tamunodukobipi, D. T. I., & Inegiyemiema, M. (2022). Comparative analysis of fibre rope (polyester) and steel (wire) rope for a Floating Production Storage and Offloading (FPSO) terminal. *Ocean Engineering*, *243*, 110081. https://doi.org/10.1016/j.oceaneng.2021.110081

Vannucchi de Camargo, F., Marcos Guilherme, C. E., Fragassa, C., & Pavlovic, A. (2016). Cyclic stress analysis of polyester, aramid, polyethylene and liquid crystal polymer yarns. *Acta Polytechnica*, *56*(5), 402–408. https://doi.org/10.14311/AP.2016.56.0402

Vlasblom, M., Boesten, J., Leite, S., & Davies, P. (2012). Development of HMPE fiber for permanent deepwater offshore mooring. In *Offshore Technology Conference* (pp. OTC-23333). OTC. https://doi.org/10.4043/23333-MS

Vlasblom, M., Engels, T., & Humeau, C. (2017). Tension endurance of HMPE fiber ropes. In *Oceans 2017-Aberdeen* (pp. 1-8). IEEE. https://doi.org/10.1109/OCEANSE.2017.8084939

Weller, S. D., Johanning, L., Davies, P., & Banfield, S. J. (2015). Synthetic mooring ropes for marine renewable energy applications. *Renewable energy*, *83*, 1268-1278. https://doi.org/10.1016/j.renene.2015.03.058

Xu, S., Wang, S., Liu, H., Zhang, Y., Li, L., & Soares, C. G. (2021). Experimental evaluation of the dynamic stiffness of synthetic fibre mooring ropes. *Applied Ocean Research*, *112*, 102709. https://doi.org/10.1016/j.apor.2021.102709

Zhao, L., Xu, L., Han, Y., Jing, H., & Gao, Z. (2019). Modelling creep-fatigue behaviours using a modified combined kinematic and isotropic hardening model considering the damage accumulation. *International Journal of Mechanical Sciences*, *161*, 105016. https://doi.org/10.1016/j.ijmecsci.2019.105016